Proc. Natl. Acad. Sci. USA
Vol. 81, pp. 4632–4636, August 1984
Biochemistry

Evidence for the existence of stable curvature of DNA in solution

(DNA structure/palindromes/differential decay of birefringence/purine clash/trypanosome)

PAUL J. HAGERMAN

Department of Biochemistry, Biophysics and Genetics, University of Colorado School of Medicine, Denver, CO 80262

Communicated by Robert L. Baldwin, March 21, 1984

ABSTRACT **A 121-base-pair DNA restriction fragment derived from the kinetoplast minicircle, Lt19, of *Leishmania tarentolae* displays substantially abnormal electrophoretic behavior on polyacrylamide gels. The electrophoretic behavior of a series of palindromic dimers containing all or part of the 121-base-pair fragment has been used to establish that curvature of the DNA helix is the basis of the abnormal behavior. One of the palindromic dimers, KP242, has been examined in more detail by using the technique of differential decay of birefringence (DDB). The technique consists of analyzing the difference in the rates of decay of birefringence for two DNA fragments, each consisting of an identical number of base pairs, and is capable of resolving differences in length as small as 1%. This approach has yielded an estimate for the apparent curvature of the dimer which, when represented as an equivalent rod with a single bend at its center, equals approximately 52°. DDB measurements made at several ionic strengths indicate that a substantial portion of the curvature is static, rather than a simple consequence of increased flexibility.**

Over the past several years, a wealth of information pertaining to the detailed structure of double-helical DNA has become available, due in large part to the successful analysis of several oligonucleotide duplexes by single-crystal x-ray diffraction methods. In their investigation of the dodecamer C-G-C-G-A-A-T-T-C-G-C-G, Wing *et al.* (1) noted that the double helical structure was associated with significant curvature. As noted by those authors, and subsequently by Dickerson *et al.* (2), such curvature may be influenced by various constraints introduced during crystallization. However, the primary basis for such curvature, namely, interstrand purine clash (3), is believed to be a fundamental property of the helix and should, therefore, be detectable in solution under appropriate conditions.

The suggestion that sequence-dependent curvature of DNA does exist in solution has come from studies of certain restriction fragments derived from kinetoplast (k) minicircles of the trypanosomatid *Leishmania tarentolae* (Lt). Simpson (4) noted that certain kDNA fragments behave abnormally (reduced electrophoretic mobility for size) on polyacrylamide gels, although their behavior is normal on agarose gels. Englund and co-workers (5, 6) made similar observations and proposed that this anomalous electrophoretic behavior is due to an unusual, perhaps bent, DNA structure. Marini *et al.* (7) have ruled out the presence of secondary structure associated with single-stranded DNA, and they have excluded bound protein or *in vivo* modifications as causes of the abnormal electrophoretic behavior. Those authors have also presented circular dichroism data which suggest that the structure of their kDNA fragment is essentially normal B-form helix.

The major aim of the present work is to identify the structural feature of kDNA that gives rise to its abnormal electrophoretic behavior. Evidence is presented which establishes that certain specific regions of a particular minicircle, Lt19 (8), do indeed possess significant curvature and, moreover, that a substantial portion of this curvature is static, not simply a manifestation of increased flexibility. It is demonstrated that a plausible explanation for the observed curvature is provided by the "purine-clash" model of Calladine (3, 9), which states that local deformations of the double helix occur as a simple consequence of cross-chain repulsive interactions between purines in adjacent base pairs.

MATERIALS AND METHODS

Plasmids. pXH7 is a pBR325 derivative that contains a 242-base-pair (bp) insert (derived from ϕX174), here designated XH242, at the *Eco*RI site (10). The plasmid-containing bacterial host, *Escherichia coli* HB101/XH7, was kindly provided by D. Shore. pLt19 is a pBR325 derivative containing two copies of a unit-length *Bam*HI-linearized, kinetoplast minicircle from *L. tarentolae* (8). The plasmid-containing host, *E. coli* RR1/pLt19, was kindly provided by L. Simpson. The cloned unit-length minicircle DNA has been designated Lt19 and has been completely sequenced (8).

Isolation of Plasmid DNA. Plasmid DNA was isolated according to the high-density fermentor protocol of Sadler (11) with the following significant modifications: (*i*) The chromosomal DNA pellet was discarded after the cleared-lysate spin. (*ii*) After resuspension of the polyethylene glycol/DNA pellet, the solution was extracted several times with chloroform prior to the usual phenol/chloroform extraction. (*iii*) The CsCl/ethidium bromide banding step was eliminated.

Preparative Isolation of Restriction Fragments. Preparative isolations typically utilized 20–50 mg of plasmid DNA, which was digested with *Eco*RI or *Bam*HI (0.5–2 units of enzyme per μg of DNA) for 2–6 hr at 37°C under standard enzyme buffer conditions. Reactions were terminated by extraction with phenol/chloroform followed by precipitation with ethanol. DNA (plasmid + insert) was loaded onto a preparative, continuous-elution, polyacrylamide gel column (>50 mg capacity) designed in the author's laboratory (to be described elsewhere). Column fractions containing the insert were pooled and passed over a DEAE-cellulose (Whatman DE52) column for concentration and further purification of the insert. Restriction fragments were stored as isopropyl alcohol slurries at −20°C until further use. The preparative gel column was also used to isolate the various reconstructed fragments used in this study.

Enzymes. *Eco*RI, *Bam*HI, and T4 DNA ligase were prepared according to published procedures. *Hae* III, *Dde* I, and *Sau*3A were purchased from Bethesda Research Laboratories.

Characterization of the Physical State of the Fragments Used in This Study. Reconstructed fragments were subjected to alkaline agarose gel electrophoresis to establish the ab-

The publication costs of this article were defrayed in part by page charge payment. This article must therefore be hereby marked "*advertisement*" in accordance with 18 U.S.C. §1734 solely to indicate this fact.

Abbreviations: kDNA, kinetoplast DNA; bp, base pair(s) (formally, number of bases per molecule divided by two); DDB, differential decay of birefringence.

sence of nicks, sites of depurination or depyrimidination, or incomplete ligation. The integrity of the ends of the various DNA molecules was verified by ligation and subsequent cleavage with the appropriate restriction enzyme. These control studies were also performed after the DNA molecules had been used for birefringence measurements. Under the conditions employed in this study, there was no detectable degradation of DNA structure, nor was there any incomplete ligation in the construction of the palindromic fragments.

Electric Birefringence Measurements. All measurements were performed with a dual-beam birefringence instrument designed by the author (12). The temperature rise in the cell during any measurement or set of measurements was always less than 50 millidegrees. The cell temperature was maintained at 3.0 ± 0.05°C. Under the conditions employed in this study, the terminal rates of birefringence decay were independent of the configuration of the pulse and were independent of DNA concentration. The overall system response time is less than 100 nsec.

RESULTS

A 121-bp *Eco*RI/*Hae* III kDNA Fragment from Lt19 Displays Significantly Abnormal Electrophoretic Behavior on Polyacrylamide Gels. The electrophoretic behavior of a number of restriction fragments of Lt19 is presented in Fig. 1. These data suggest that essentially all of the abnormal behavior is dependent upon sequences lying within an approximately 250-bp conserved region of Lt19, in agreement with the results of Kidane *et al.* (8). Furthermore, inspection of Fig. 1 reveals that sequences giving rise to the anomalous electrophoretic behavior are distributed over at least 60 bp within the conserved region. It should also be noted that kDNA fragments consisting of fewer than 100 bp were still capable of manifesting abnormal electrophoretic behavior on 9% polyacrylamide gels. One kDNA restriction fragment, namely, the 121-bp *Eco*RI/*Hae* III fragment, was chosen for further study, on the basis of (*i*) its abnormal electrophoretic behavior, (*ii*) the presence of different restriction enzyme termini, and (*iii*) the presence of suitably placed internal restriction sites.

The Electrophoretic Behavior of a Series of Palindromic Molecules Derived from the 121-bp *Eco*RI/*Hae* III Fragment Provides Direct Evidence for Curvature Within That Fragment. The sequences of interest have been further characterized by constructing a series of DNA molecules that are palindromic with respect to various restriction sites associated with the 121-bp *Eco*RI/*Hae* III fragment (Fig. 2). Several conclusions can be drawn from the electrophoretic behavior of these palindromes. (*i*) The fact that the two 242-bp kDNA palindromes (identical molecular weight and base composition) differ markedly in electrophoretic mobility immediately rules out simple base-composition effects (including base modifications) as well as simple solenoidal effects (i.e., changes in helical structure that preserve the overall linearity of the helix). (*ii*) The abnormal behavior is not a consequence of secondary structure (i.e., cruciform) formation in the palindromic molecules, since a heterotypic "dimer" consisting of a 100-bp *Hae* III/*Eco*RI fragment derived from phage ϕX174 plus a 121-bp *Eco*RI/*Hae* III kDNA fragment, ligated across the *Eco*RI site, also displays significantly abnormal electrophoretic behavior (data not shown). This observation is consistent with the observations of Marini *et al.* (7), who failed to detect any secondary structural elements in their kinetoplast fragment, which, after redetermination of the sequence, is known to be identical in sequence to the 410-bp *Sau*3A fragment of Lt19 (7, 13). This conclusion provides direct evidence in support of the proposal that a bent helical structure exists in kDNA. (*iii*) The observation that both 242-bp kDNA fragments migrate abnormally rules out a sharp bend at either the *Eco*RI site or the *Hae* III site, a result that is not surprising since neither site is associated with abnormal electrophoretic behavior in nonkinetoplast DNA. (*iv*) The essentially normal behavior of the 238-bp *Bam*HI/*Eco*RI fragment as well as both of its palindromic dimer counterparts (data not shown) suggests that the region of curvature lies mainly to the right of the *Eco*RI site. (*v*) The markedly abnormal behavior of the 123-bp *Dde* I palindrome, coupled with the relatively normal behavior of its 119-bp complement, further suggests that most of the curvature of the helix resides within the 61.5-bp (58 paired bases + 7 unpaired bases forming the two tails) *Eco*RI/*Dde* I frag-

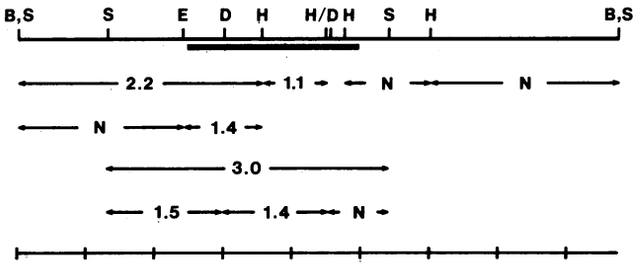

FIG. 1. Partial restriction map of the cloned kinetoplast minicircle Lt19 derived from the trypanosome *L. tarentolae*. The numbers associated with various restriction fragments refer to the ratio of the apparent molecular weights of the fragments, as determined on 9% polyacrylamide gels (acrylamide-to-bisacrylamide ratio, 38:1; running buffer, 40 mM Tris acetate/20 mM sodium acetate/1 mM Na_2-EDTA, pH 7.9, room temperature), to their true molecular weights based on sequence (8). DNA fragments migrating with apparent molecular weights within 5% of their true molecular weights are indicated by N. The heavy bar refers to a region of substantial sequence homology between Lt19 and other kinetoplast minicircles from *L. tarentolae* (8). For the scale at the bottom of the figure, the separation between vertical bars is 100 bp. B, *Bam*HI; S, *Sau*3A; E, *Eco*RI; D, *Dde* I; H, *Hae* III.

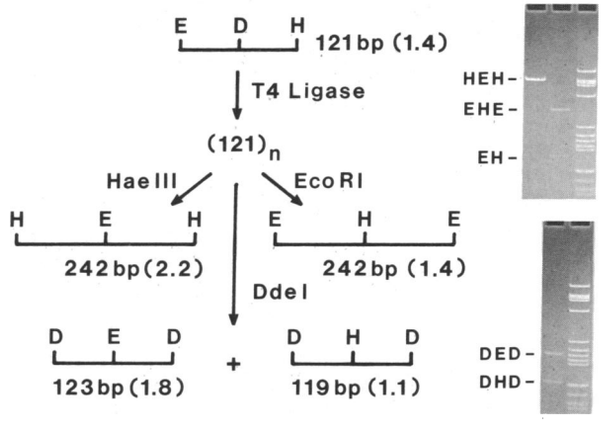

FIG. 2. Outline of the construction and gel electrophoretic behavior of several derivatives of the 121-bp *Eco*RI/*Hae* III fragment from Lt19 (Fig. 1). The 121-bp fragment was converted to higher-order multimers by overnight ligation with T4 DNA ligase (0.02 unit/μg of DNA) at 16°C (ligation buffer: 50 mM Tris·HCl/10 mM $MgCl_2$/20 mM dithiothreitol/1.0 mM ATP, pH 8.0). The reaction was stopped by heating to 65°C for 10 min. After cooling to 37°C, the reaction mix was diluted 1:5 and supplemented with the appropriate enzyme buffer prior to the addition of restriction enzymes. All digestions were carried out with excess enzyme (>1 unit/μg of DNA) for approximately 4 hr. Reactions were terminated by extraction with phenol/ether followed by precipitation with isopropyl alcohol. All gels contain a *Hae* III digest of pBR322 for reference (right lanes). The 242-bp palindrome HEH has also been designated KP242 (see text) and was used for subsequent birefringence measurements. Ratios of apparent molecular weights to true molecular weights are given in parentheses.

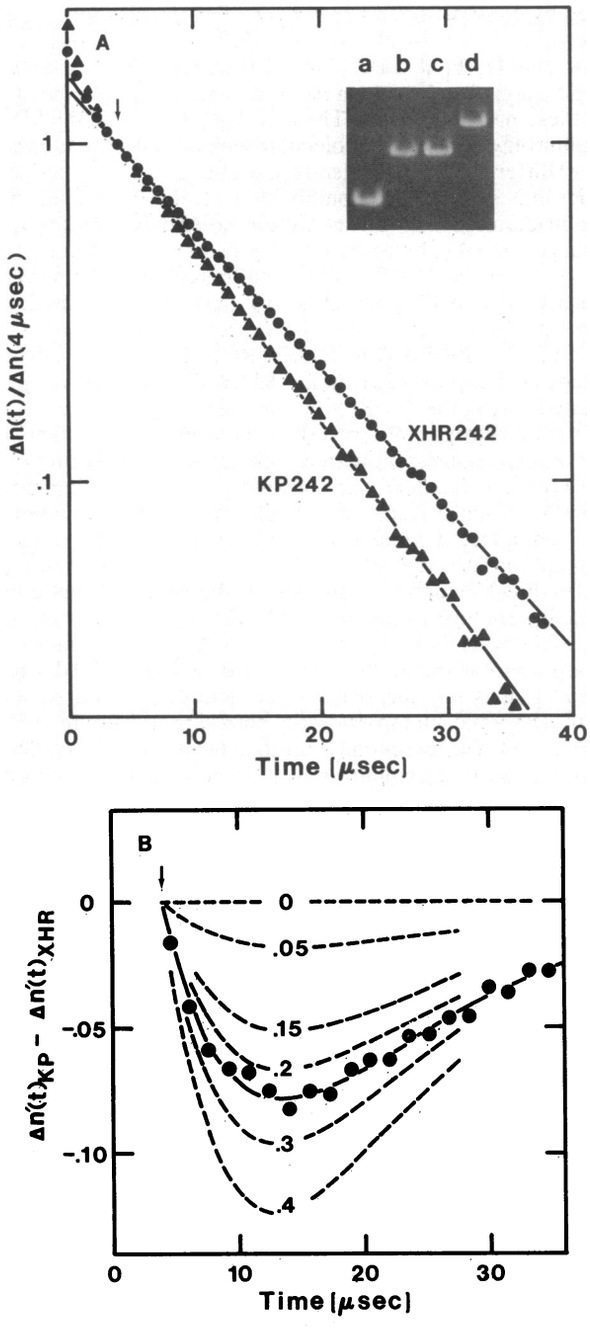

FIG. 3. (*A*) Semilogarithmic plots of the decay of birefringence (n) for the two 242-bp fragments, KP242 and XHR242. Buffer composition: 1.0 mM Tris·HCl, pH 8.0/0.1 mM $MgCl_2$. This buffer was chosen to maximize the birefringence signal while minimizing the electrostatic contribution to the persistence length (14). The birefringence decay curves have each been normalized with respect to their respective birefringence signals 4 μsec after removal of the electric field (descending arrow). The portion of each curve corresponding to $t < 4$ μsec displays a small fast component and is therefore excluded from the subsequent analysis of DDB. (*Inset*) Alkaline agarose gel (2.0%) of KP242 (lane b). Other lanes include 98-bp marker (lane a), XH242 (lane c), and 366-bp marker (lane d). This control gel was run with KP242 that had been subjected to DDB measurements. Single-stranded half-molecules would have appeared slightly above the position of the 98-base fragment in lane a. (*B*) Plot of DDB using the prenormalized curves from A [$\Delta n'(t) = \Delta n(t)/\Delta n(4\ \mu\text{sec})$]. The filled circles have been obtained by subjecting the primary difference curve to a 3-point averaging procedure. The broken lines represent expected difference curves for various values of R [$= (\tau_{XHR}/\tau_{KP}) - 1$] as indicated. The solid line represents a least-squares best fit to the experimental difference curve ($R = 0.24 \pm 0.01$). The uncertainty in R ($\pm$ 0.01) represents the combined standard error obtained from the single-parameter (R) fit displayed in B and the initial determination of τ_{XHR}. A 5% uncertainty in the value of τ_{XHR} would lead to a 1.7% uncertainty in R. The overall standard error corresponds to a difference in length between two straight rods of 0.3%, thus underscoring the extreme precision of the DDB approach. The bend angle for an equivalent once-bent rod was determined by interpolation from table 2 of ref. 15, using the formula $R = D - (B/3) - 1$, in which $D = (D_x + D_y + D_z)/3$ and $B = (D_x^2 + D_y^2 + D_z^2 - D_xD_y - D_xD_z - D_yD_z)^{1/2}$ (16), and D_x, D_y, and D_z are the three principal diffusion coefficients for the bent rod (15).

ment, although a small amount of curvature in the *Dde* I/*Hae* III fragment cannot be ruled out.

It should be noted that abnormal electrophoretic mobility does not necessarily imply *static* curvature. Such abnormal behavior might arise as a consequence of a region of markedly increased flexibility. This ambiguity will be considered further below.

Estimation of the Apparent Curvature of the 242-bp Fragment KP242, Using the Technique of Differential Decay of Birefringence (DDB). The 242-bp palindrome containing a central *Eco*RI site (designated KP242; Fig. 2) has proven to be a suitable starting point for the study of curvature for the following three reasons: (*i*) the molecule is sufficiently small to facilitate the study of structure with only a relatively minor contribution due to the flexibility of the helix (14); (*ii*) the electrophoretic mobility of KP242 is markedly abnormal (Fig. 2); and (*iii*) an unrelated 242-bp, blunt-ended DNA molecule derived from XH242 by inversion about an internal *Alu* I site (designated XHR242), which displays normal electrophoretic behavior, can be prepared easily.

By comparing the rotational diffusion of the two DNA molecules, KP242 and XHR242, an estimate of the apparent curvature of KP242 can be made. This comparison was performed by analyzing the difference in the rates of decay of birefringence [designated DDB (12)]. With this method, differences in length as small as 1% can be detected (Fig. 3). The results of the DDB analysis for one set of buffer conditions is displayed in Fig. 3. For this example, the ratio of the birefringence decay times is $\tau_{XHR}/\tau_{KP} = 1.24 \pm 0.01$. For a rigidly bent rod with a single sharp bend at its center, this ratio corresponds to a bend angle of 52° ± 2°. An estimate of the effect of residual flexibility on the difference analysis, based on the formulas of Hagerman and Zimm (17), indicates that such effects would alter the apparent bend angle by only a few degrees. The true curvature is undoubtedly distributed over a substantial portion of the molecule, and may not be confined to a single plane.

A Substantial Portion of the Curvature Present in KP242 Is Static. The measurements depicted in Fig. 3 were made in the presence of 0.1 mM $MgCl_2$, which essentially eliminates electrostatic contributions to the persistence length (P) of DNA (14). Under those conditions, if *all* of the difference between τ_{KP} and τ_{XHR} were due to a uniform reduction in the value of P associated with KP242, the resulting value of P would be 325 Å ($P_{XHR} \approx 500$ Å). As the ionic strength of the solutions used in the DDB measurements is decreased to the point at which electrostatic contributions to P predominate, R [$= (\tau_{XHR}/\tau_{KP}) - 1$] should approach zero. For example, the expected value of R at 0.1 mM ionic strength would be *ca.* 0.01 (14). As can be seen by inspection of Table 1, R is substantially larger than 0.01 under those conditions. The gradual drop in R values may reflect either a small difference in P between P_{KP} and P_{XHR} or, more likely, a gradual repulsion of the ends of the curved molecule.

The Purine-Clash Model of Calladine Provides a Plausible Molecular Basis for the Curvature of kDNA in Solution. To test the plausibility of the hypothesis that purine clash (3) is responsible for the curvature observed in kDNA, contours representing the helix axis (Fig. 4) were generated by using

Table 1. Dependence of DDB on buffer composition for the two fragments KP242 and XHR242

Buffer	R^*
0.1 mM NaCl/0.001 mM Na_2EDTA	0.12
0.3 mM NaCl/0.003 mM Na_2EDTA	0.17
1.0 mM NaCl/0.01 mM Na_2EDTA	0.21
1.0 mM Tris·HCl, pH 8.0/0.10 mM $MgCl_2$†	0.24

*$R = (\tau_{XHR}/\tau_{KP}) - 1$.
†Presented in Fig. 4.

the set of rules proposed by Dickerson (9) with one significant modification—namely, the removal of compensatory roll at positions adjacent to the central base pair transition, as suggested by Dickerson (R. Dickerson, personal communication). This modification should provide a somewhat better representation of the "native" helix, since the sum functions were developed for the self-compensating MPD7 helix (9-Br derivative soaked in methylpentanediol at 7°C), which has undergone a transition from a helix with curvature to a straight helix (1, 18). The contour of the KP242 helix is only marginally influenced by the mode of compensation of local twist (data not shown), suggesting that the sequence dependence of curvature is primarily determined by locally uncompensated roll. It should be noted that the fully compensating sum functions proposed by Dickerson (9) were designed to yield a straight helix, in conformance with the structure of the MPD7 helix, upon which they are based. In view of the caveats associated with a direct comparison of the crystal and solution forms of the DNA helix, no attempt has been made to obtain a "best fit" for twist and roll angles at this point, the purpose of Fig. 4 being simply to demonstrate the plausibility of the purine-clash model as a basis for the observed curvature of kDNA in solution.

DISCUSSION

Evidence has been presented that establishes the existence of static, sequence-dependent curvature of DNA in solution. Substantial curvature of a duplex DNA dodecamer in crystalline form had been observed previously (1). The proposed basis for the curvature of the dodecamer—namely, interstrand purine clash (3, 9)—leads to the prediction that such curvature should also exist in solution. The present study confirms this prediction. Although it has not been established that the observed curvature of DNA in solution is, in fact, a direct consequence of purine clash, application of the modified sum functions of Dickerson (ref. 9; Fig. 4) leads to estimates of curvature for KP242 in reasonable agreement with the results of DDB measurements (Fig. 3).

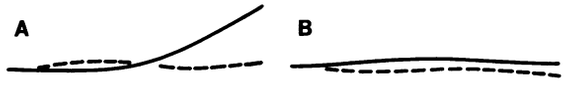

FIG. 4. Predicted contours for KP242 (*A*) and XHR242 (*B*), based on modified rules for cross-chain purine clash (detailed definitions of the sum functions as well as for twist and roll are given in refs. 9 and 18). In the present analysis, the magnitudes of the contributions to twist and roll due to purine clash are those of Dickerson (9) with the following exception: compensatory roll at positions adjacent to the central purine–pyrimidine (or pyrimidine–purine) transition has been eliminated (see text). Solid lines, *x*–*z* plane; broken lines, *x*–*y* plane. The transformation matrix used in this study has been presented elsewhere (17). The use of the solution value of 10.4 bp per turn (19), both for locally compensated and for locally uncompensated twist, imparts a spiral character to the contour while preserving local curvature (data not shown). As calculated by using the modified sum functions of Dickerson (9), the angle between tangents to the ends of the KP242 contour is approximately 30°C, irrespective of whether locally compensated or locally uncompensated twist is used.

An alternative model for static curvature, based on a correlation analysis of a number of sequences of eukaryotic DNA, has been proposed (6, 20), in which a slight bend occurs at positions of ApA dinucleotides. However, the crystallographic data of Dickerson fail to demonstrate any substantial roll or tilt angles associated with either of the ApA dinucleotides present in the dodecamer, rendering this model unlikely as a source of significant static curvature. Further evidence that militates against the ApA model comes from studies (unpublished results) of a 415-bp *Tha* I fragment derived from *Paramecium* mitochondrial DNA (21). This molecule consists of 96% A·T base pairs, and it migrates on 9% polyacrylamide gels with an apparent size only 16% higher than its size based on sequence; the 410-bp *Sau*3A fragment (Fig. 1) migrates with an apparent molecular weight 3 times its size based on sequence. Using the angle of 5° per ApA dinucleotide proposed by Levene and Crothers (22), the 415-bp mitochondrial DNA fragment is predicted to be dramatically contorted, with an attendant 17% reduction in end-to-end separation. The end-to-end reduction predicted by using the modified sum functions is 2%. For comparison, the reductions in end-to-end separation for KP242 and XHR242, determined by using the modified sum functions, are 3% and 0.5%, respectively. The observation (20) of the approximately 10.5-bp periodicity of ApA dinucleotides may, in fact, reflect a reduced bending potential at those positions, thus facilitating the packaging of DNA into nucleosomes. This last proposal is in accord with the model of Zhurkin *et al.* (23).

A previous study (6) of the structure of kDNA relied on a sequence for an *Mbo* I fragment that was in error (P. Englund, personal communication; ref. 13). The correct sequence is identical to that of the largest *Sau*3A fragment of Lt19 (8) and consists of 410 bp, not 490 bp as previously reported. The Sephacryl S-500 study (6), therefore, does not demonstrate any significant filtration abnormality associated with the kDNA fragment. Moreover, those authors apparently missed the slow phase of the decay process in their dichroism measurements of the 410-bp *Sau*3A (MboI) fragment (Fig. 5). The terminal decay constant, $\tau_{410} = 23.1$ μsec (Fig. 5) is only 20–30% smaller than the value predicted (14) for a "normal" fragment of the same contour length. This result, along with the results presented in Fig. 3 and Table 1, indicates that even significant curvature is associated with relatively subtle changes in the rates of rotational diffusion

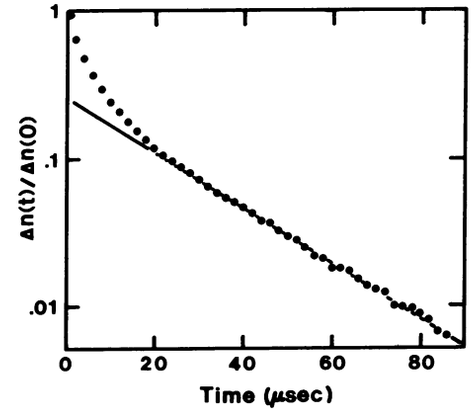

FIG. 5. Semilogarithmic plot of the decay of birefringence of the 410-bp *Sau*3A fragment from Lt19 (Fig. 1). Measurements were made in buffer having a composition identical to that of Marini *et al.* (6) (0.3 mM NaH_2PO_4/0.6 mM Na_2HPO_4). Temperature, 3.0°C. Analysis of the linear portion of the curve yields $\tau_{410} = 23.1$ μsec. A forced fit of the entire birefringence decay curve to a single exponential yields a value for $\tau_{apparent}$ of 7–10 μsec, depending upon the field strength. The decay time of the terminal portion of the curve is independent of the field strength.

and, therefore, a sensitive approach such as DDB is required.

The biological role for the curvature found associated with certain regions of the kinetoplast minicircles is unknown at present. One might surmise that such curvature is important to the organism since it appears to be localized to within conserved regions among various minicircle classes (8). However, it may turn out that it is the sequence that is important, the curvature simply being a consequence of the required sequence arrangement. Regardless of the biological role of kDNA curvature, the systematic examination of such regions of curvature should provide important clues regarding the nature of the forces governing the structure of double-helical DNA. These investigations should also provide a means by which information derived from x-ray crystallography can be related to the structure of DNA in solution.

I thank Profs. R. Dickerson, P. Englund, L. Simpson, and R. Wells for useful discussions concerning this work. I also thank each of the above individuals and Dr. A. Pritchard for providing me with copies of their manuscripts prior to publication. This research was supported by Grant 2RO1GM28293 from the National Institutes of Health.

1. Wing, R. M., Drew, H. R., Takano, T., Broka, C., Tanaka, S., Itakura, K. & Dickerson, R. E. (1980) *Nature (London)* **287,** 755–758.
2. Dickerson, R. E., Kopka, M. L. & Pjura, P. (1983) *Proc. Natl. Acad. Sci. USA* **80,** 7099–7103.
3. Calladine, C. R. (1982) *J. Mol. Biol.* **161,** 343–352.
4. Simpson, L. (1979) *Proc. Natl. Acad. Sci. USA* **76,** 1585–1588.
5. Challberg, S. S. & Englund, P. T. (1980) *J. Mol. Biol.* **138,** 447–472.
6. Marini, J. C., Levene, S. D., Crothers, D. M. & Englund, P. T. (1982) *Proc. Natl. Acad. Sci. USA* **79,** 7664–7668.
7. Marini, J. C., Effron, P. N., Goodman, T. C., Singleton, C. K., Wells, R. D., Wartell, R. M. & Englund, P. T. (1984) *J. Biol. Chem.*, in press.
8. Kidane, G. Z., Hughes, D. & Simpson, L. (1984) *Gene* **27,** 265–277.
9. Dickerson, R. E. (1983) *J. Mol. Biol.* **166,** 419–441.
10. Shore, D., Langowski, J. & Baldwin, R. L. (1981) *Proc. Natl. Acad. Sci. USA* **78,** 4833–4837.
11. Sadler, J. R. & Tecklenburg, M. (1981) *Gene* **13,** 13–23.
12. Hagerman, P. J. (1984) *Methods Enzymol.*, in press.
13. Marini, J. C., Levene, S. D., Crothers, D. M. & Englund, P. T. (1983) *Proc. Natl. Acad. Sci. USA* **80,** 7678 (correction).
14. Hagerman, P. J. (1981) *Biopolymers* **20,** 1503–1535.
15. Mellado, P. & Garcia de la Torre, J. (1982) *Biopolymers* **21,** 1857–1871.
16. Wegener, W. A., Dowben, R. M. & Koester, V. J. (1979) *J. Chem. Phys.* **70,** 622–632.
17. Hagerman, P. J. & Zimm, B. H. (1981) *Biopolymers* **20,** 1481–1502.
18. Fratini, A. V., Kopka, M. L., Drew, H. R. & Dickerson, R. E. (1982) *J. Biol. Chem.* **257,** 14686–14707.
19. Wang, J. C. (1979) *Proc. Natl. Acad. Sci. USA* **76,** 200–203.
20. Trifonov, E. N. & Sussman, J. L. (1980) *Proc. Natl. Acad. Sci. USA* **77,** 3816–3820.
21. Pritchard, A. E. & Cummings, D. J. (1983) *UCLA Symposium on Molecular and Cellular Biology*: New Series, ed. Cozzarelli, N. R. (Liss, New York), Vol. 10, pp. 595–604.
22. Levene, S. D. & Crothers, D. M. (1983) *J. Biomol. Struct. Dyn.* **1,** 429–435.
23. Zhurkin, V. B., Lysov, Y. P. & Ivanov, V. I. (1979) *Nucleic Acids Res.* **6,** 1081–1096.